

# USED FUEL DISPOSITION CAMPAIGN

## *Effect of Iron on Radiolytic Hydrogen Peroxide Generation*

**Fuel Cycle Research & Development**

*Prepared for  
U.S. Department of Energy  
Used Fuel Disposition  
Campaign*

*Edgar Buck  
Rick Wittman*

*July 29, 2016*

M4FT-16PN080303072

PNNL-25639



Disclaimer

This information was prepared as an account of work sponsored by an agency of the U.S. Government. Neither the U.S. Government nor any agency thereof, nor any of their employees, makes any warranty, expressed or implied, or assumes any legal liability or responsibility for the accuracy, completeness, or usefulness, of any information, apparatus, product, or process disclosed or represents that its use would not infringe privately owned rights. References herein to any specific commercial product, process, or service by trade name, trade mark, manufacturer, or otherwise, does not necessarily constitute or imply its endorsement, recommendation, or favoring by the U.S. Government or any agency thereof. The views and opinions of the authors expressed herein do not necessarily state or reflect those of the U.S. Government or any agency thereof.

**Submitted by:**

Signature on file

---

Edgar C. Buck  
PNNL



## EXECUTIVE SUMMARY

This report fulfills the M4FT-16PN080303072 to report on continuing the model integration of the PNNL Radiolysis Model and the ANL Mixed Potential Model for Crystalline Disposal. In this work we demonstrate and approximate possible effects of iron from corrosion of surrounding structures on hydrogen peroxide generation. We find that even small concentrations of Fe(II) reduces the steady-state  $H_2O_2$  concentration.

Additionally, suggestions are offered on what further data or measurements would be required for model verification and applicability. The Listings of the reactions considered in this report are given in Appendix.



## ACKNOWLEDGMENTS

We thank Jim Jerden and Bill Ebert for helpful discussions on the operation of the ANL Mixed Potential Model and proposing the definition of a conditional  $G$ -value. We thank Carlos Jové-Colón, and David Sassani for support and helpful discussions on the effects of iron chemistry and its applicability to model predictions.





## CONTENTS

EXECUTIVE SUMMARY .....	v
ACKNOWLEDGMENTS .....	vii
CONTENTS.....	ix
ACRONYMS.....	xi
1. INTRODUCTION.....	13
2. RADIOLYSIS MODEL WITH IRON REACTIONS.....	15
2.1 Effect of Iron on H <sub>2</sub> O <sub>2</sub> in Radiation Zone.....	15
2.2 Future work.....	18
3. REFERENCES .....	19
APPENDIX A: Reaction Listing for Full RM .....	20

## FIGURES

Figure 2-1. Effect of an initial micro-molar concentration of Fe(II) on H<sub>2</sub>O<sub>2</sub> generation. Comparison of with and without dose rate (red and black). Comparison of with and without Fe(II) (solid and dashed curves). ..... 16

Figure 2-2. Concentrations of Fe(II), Fe(III) and O<sub>2</sub><sup>-</sup> during H<sub>2</sub>O<sub>2</sub> decomposition..... 18

## TABLES

Table 2-1. Subset of reactions sufficient to represent the primary mechanisms for H<sub>2</sub>O<sub>2</sub> generation in the full RM (Appendix A) [Iron from Ref. (De Laat, et al., 1999)]. ..... 17

## ACRONYMS

ANL	Argonne National Laboratory
DOE	U.S. Department of Energy
DOE-NE	U.S. Department of Energy Office of Nuclear Energy
MPM	Mixed Potential Model
ODE	ordinary differential equation
PNNL	Pacific Northwest National Laboratory
RM	Radiolysis Model
SNF	spent nuclear fuel
UFDC	Used Fuel Disposition Campaign
UNF	used nuclear fuel



# USED FUEL DISPOSITION CAMPAIGN

## Effect of Iron on Radiolytic Hydrogen Peroxide Generation

### 1. INTRODUCTION

The U.S. Department of Energy Office of Nuclear Energy (DOE-NE), Office of Fuel Cycle Technology has established the Used Fuel Disposition Campaign (UFDC) to conduct the research and development activities related to storage, transportation, and disposal of used nuclear fuel (UNF) and high-level radioactive waste. Within the UFDC, the components for a general system model of the degradation and subsequent transport of UNF is being developed to analyze the performance of disposal options [Sassani et al., 2012]. Two model components of the near-field part of the problem are the ANL Mixed Potential Model and the PNNL Radiolysis Model.

This report is in response to the desire to integrate the two models as outlined in [Buck, E.C, J.L. Jerden, W.L. Ebert, R.S. Wittman, (2013) "Coupling the Mixed Potential and Radiolysis Models for Used Fuel Degradation," FCRD-UFD-2013-000290, M3FT-PN0806058]

This report gives the details on the effect of iron chemistry on  $H_2O_2$  decomposition under radiolytic condition at the surface of used nuclear fuel under repository conditions. Additionally, suggestions are offered on what further data or measurements would be required for model verification and applicability. The Listings of the reactions considered in this report are given in Appendix.



## 2. RADIOLYSIS MODEL WITH IRON REACTIONS

Previous work that reports the results of a radiolysis model sensitivity study [Wittman RS and EC Buck. 2012] showed that of the approximately 100 reactions [Pastina, B. and LaVerne, J. A., 2001] describing water radiolysis, only about 37 are required to accurately predict  $H_2O_2$  to one part in  $10^5$ . The intended application of that radiolysis model (RM) was to calculate  $H_2O_2$  production for an electrochemical based mixed potential model (MPM) [Jerden, J., Frey, K., Cruse, T., and Ebert, W., 2013] developed to calculate the oxidation/dissolution rate of used nuclear fuel [Shoosmith, D.W., Kolar, M., and King, F., 2003] under disposal conditions where  $O_2$  is expected to be at low concentrations and  $H_2$  is generated from oxidation of steel containers.

As an initial approximation, that model (MPM) was developed under the assumption that  $H_2O_2$  is generated at a rate determined only by its radiolytic  $G$ -value. Ideally, for a full RM-MPM integration, the MPM would use a reaction kinetics based model to predict  $H_2O_2$  for various water chemistries. As a further step in that direction, this report presents the effect of small concentration of [Fe(II)] on  $H_2O_2$  concentration and explains the mechanism of that effect.

### 2.1 Effect of Iron on $H_2O_2$ in Radiation Zone

To better understand how integration of the PNNL Radiolysis Model (RM) can be integrated with the ANL Mixed Potential Fuel Degradation Model in the environment of iron containing species we consider iron reactions in the RM. Since our goal is to consistently account for the chemistry in both models we focus on the mechanism and effect of iron on prediction  $H_2O_2$  decomposition affecting the  $UO_2$  degradation rate.

The main approach is as follows.

- Identify the significant reactions that govern the chemical and radiolytic decomposition of  $H_2O_2$  in water with known dose rate and concentrations of iron species (De Laat, et al., 1999 and Bouniol, 2010).
- Determine if iron chemistry is well understood enough to accurately represent its effects on decomposition of  $H_2O_2$  in the RM.

Progress on Bullet one (above) is summarized here and Bullet two is left as an open question.

Figure 1 of reference (De Laat, et al., 1999) was reproduced by our current kinetics model as a check of the numerical solution and our understanding of the model definition. Assuming 38 water reactions from previous radiolysis model work (Wittman and Buck 2012) and approximately 60 additional iron containing reactions of Refs. (De Laat, et al., 1999 and Bouniol, 2010) we initially find that approximately 60 total reactions are sufficient to reproduce the  $H_2O_2$  concentration.

Figure 1 shows both the radiolytic and iron concentration effects on the  $H_2O_2$  concentration. Without dose, the initial 0.01 molar  $H_2O_2$  concentration is initially catalytically decomposed at a rate of 160 times faster than thermal decomposition ( $25^\circ$ ) alone. Additionally, at a dose rate of 25 krad/s the steady-state  $H_2O_2$  concentration is about 160 times lower with an initial  $1 \mu M$  concentration of Fe(II) that is converted to  $1 \mu M$  of Fe(II). For these comparisons pH is fixed at 7.0 and no constraints were put on oxygen and hydrogen concentrations. The effect of those constraints with diffusion out of the alpha radiation zone is currently being explored. Further work is in progress to confirm the applicability of the reaction kinetics for pH and iron concentrations required by Mixed Potential  $UO_2$  Fuel Degradation Model. Also, further work is in progress to confirm the applicability of the reaction kinetics for pH and iron concentrations required by Mixed Potential  $UO_2$  Fuel Degradation Model.

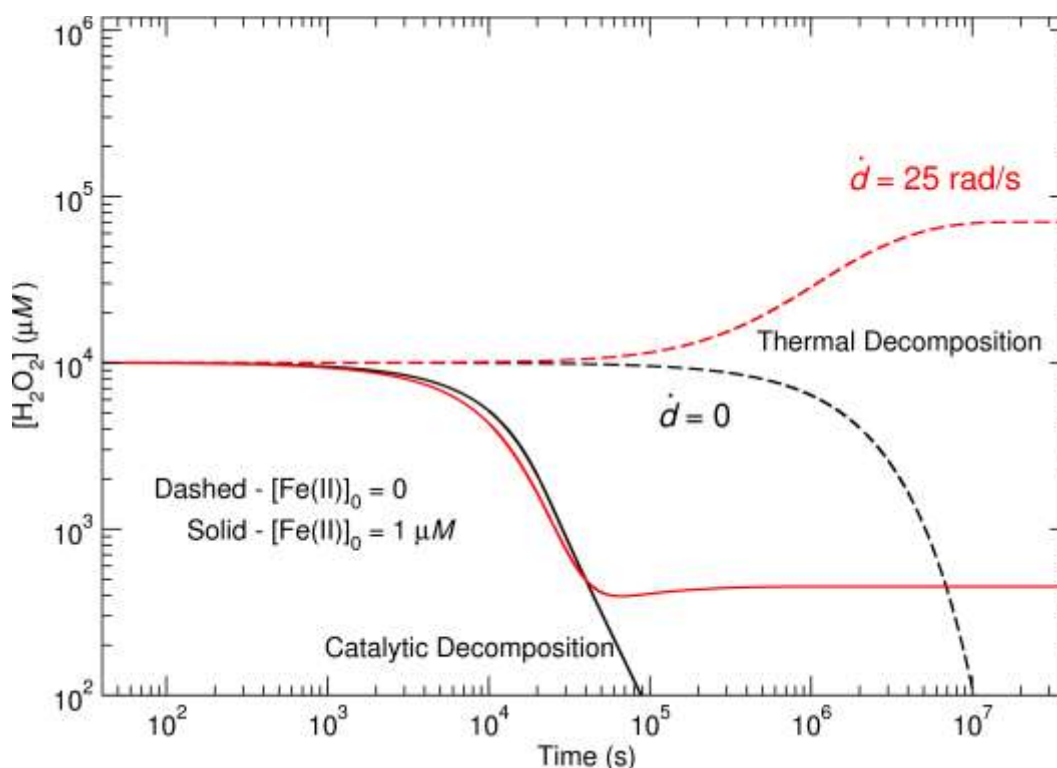


Figure 2-1. Effect of an initial micro-molar concentration of Fe(II) on  $H_2O_2$  generation. Comparison of with and without dose rate (red and black). Comparison of with and without Fe(II) (solid and dashed curves).

Table 2-1 was found to be a sufficient set of reactions to describe the main features of Figure 1 and contains the mechanism that  $H_2O_2$  decomposes or shifts its steady-state concentration. The main process responsible for  $H_2O_2$  decomposition is Fenton's reaction (51 of Table 2-1) (Fenton, H.J.H., (1894) where Fe(II) attains a secular equilibrium with a lower concentration of Fe(III). The effective equilibrium arises because  $\cdot OH$  radicals react with water forming  $O_2^-$  which reduces Fe(III) back to Fe(II) (58 and 60 of Table 2-1).



Table 2-1. Subset of reactions sufficient to represent the primary mechanisms for H<sub>2</sub>O<sub>2</sub> generation in the full RM (Appendix A) [Iron from Ref. (De Laat, et al., 1999)].

	Reaction	$k_r$
3	$\text{H}_2\text{O}_2 \rightarrow \text{H}^+ + \cdot\text{HO}_2^-$	$1.1 \times 10^{-1}$
4	$\text{H}^+ + \cdot\text{HO}_2^- \rightarrow \text{H}_2\text{O}_2$	$5.0 \times 10^{10}$
15	$\cdot\text{HO}_2 \rightarrow \text{O}_2^- + \text{H}^+$	$1.3 \times 10^6$
16	$\text{O}_2^- + \text{H}^+ \rightarrow \cdot\text{HO}_2$	$5.0 \times 10^{10}$
23	$e^- + \text{H}_2\text{O}_2 \rightarrow \cdot\text{OH} + \text{OH}^-$	$1.1 \times 10^{10}$
26	$\cdot\text{H} + \text{H}_2\text{O}_2 \rightarrow \cdot\text{OH} + \text{H}_2\text{O}$	$9.0 \times 10^7$
27	$\cdot\text{H} + \text{O}_2 \rightarrow \cdot\text{HO}_2$	$2.1 \times 10^{10}$
33	$\cdot\text{OH} + \text{H}_2 \rightarrow \cdot\text{H} + \text{H}_2\text{O}$	$4.3 \times 10^7$
34	$\cdot\text{OH} + \text{H}_2\text{O}_2 \rightarrow \cdot\text{HO}_2 + \text{H}_2\text{O}$	$2.7 \times 10^7$
35	$\cdot\text{HO}_2 + \text{O}_2^- \rightarrow \cdot\text{HO}_2^- + \text{O}_2$	$8.0 \times 10^7$
36	$\text{H}_2\text{O}_2 \rightarrow \cdot\text{OH} + \cdot\text{OH}$	$2.5 \times 10^{-7}$
41	$\text{Fe}^{3+} + 2\text{H}_2\text{O} \rightarrow \text{Fe}(\text{OH})_2^+ + 2\text{H}^+$	$1 \times 10^5$
42	$\text{Fe}(\text{OH})_2^+ + 2\text{H}^+ \rightarrow \text{Fe}^{3+} + 2\text{H}_2\text{O}$	$1.3 \times 10^{11}$
51	$\text{Fe}^{2+} + \text{H}_2\text{O}_2 \rightarrow \text{Fe}^{3+} + \cdot\text{OH} + \text{OH}^-$	63.0
52	$\text{Fe}^{2+} + \cdot\text{OH} \rightarrow \text{Fe}^{3+} + \text{OH}^-$	$3.2 \times 10^8$
58	$\text{Fe}^{3+} + \text{O}_2^- \rightarrow \text{Fe}^{2+} + \text{O}_2$	$5 \times 10^7$
60	$\text{Fe}(\text{OH})_2^+ + \text{O}_2^- \rightarrow \text{Fe}^{2+} + \text{O}_2 + 2\text{OH}^-$	$5 \times 10^7$

The mechanism can be understood by focusing on a few species during H<sub>2</sub>O<sub>2</sub> decomposition (Figure 2-2). Figure 2-2 shows that without the reducing reactions (58 and 60 of Table 2-1) the Fe(II) quickly oxidized to Fe(III) resulting in little or no decomposition of H<sub>2</sub>O<sub>2</sub>. Depending on solution pH the Fe(III) will remain or precipitate from solution. The solid lines show that the iron reducing reaction create an effective fixed concentration of Fe(II) which enables decomposition – while both Fe(II) and Fe(III) participate in reactions, the Fe(II)/Fe(III) equilibrium effective acts like a catalyst. Therefore the decomposition mechanism requires the Fe(III) reduction reactions to preserve even a small concentration of Fe(II). It's this last point that make the inclusion of this mechanism unclear for the RM because if Fe(III) drops out of solution at a rate faster than it can be reduced back to Fe(II) the RM will non-conservatively predict lower than actual H<sub>2</sub>O<sub>2</sub> production rates. The current fuel degradation model assumption is that Fe(III) precipitates on formation without subsequent reduction to Fe(II). While Figure 2-2 shows that the concentration of Fe(III) is almost 10X less than Fe(II), the solubility of Fe(III) and its precipitation rate is an open question for conditions (pH, etc.) appropriate for UO<sub>2</sub> degradation.

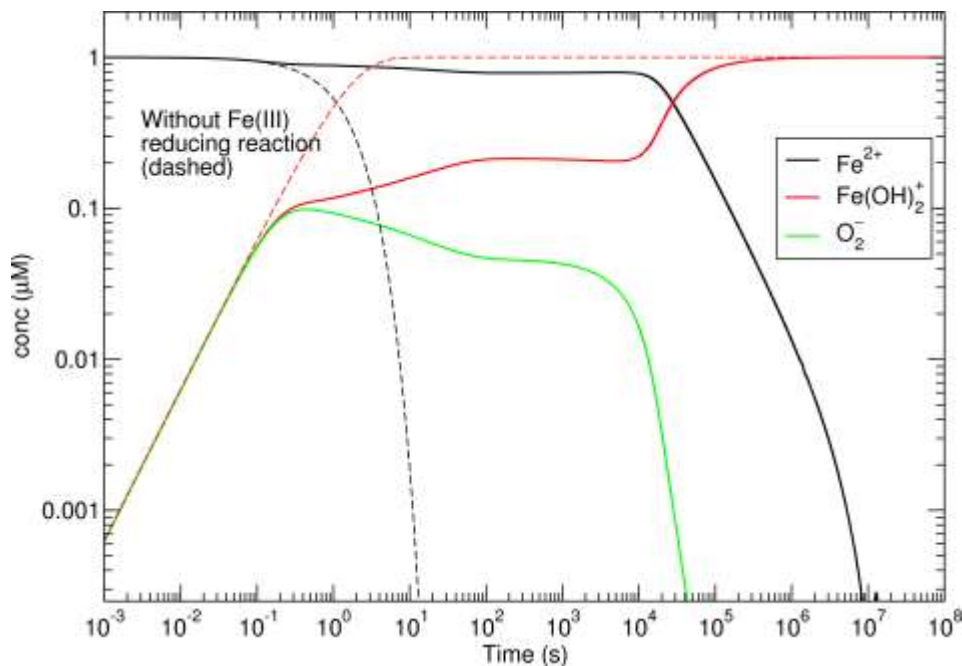


Figure 2-2. Concentrations of Fe(II), Fe(III) and  $O_2^-$  during  $H_2O_2$  decomposition.

## 2.2 Future work

While this work identifies for mechanism for an effective Fe(II)/Fe(III) equilibrium to catalytically reduce  $H_2O_2$  production rates, it cannot guarantee that the mechanism operates under the repository conditions of spent nuclear fuel. Future work that would measure Fe(III) solubility and precipitation rates, ideally under radiolytic conditions, are necessary for a confident inclusion of iron reaction in the RM.

### 3. REFERENCES

Buck, E.C, J.L. Jerden, W.L. Ebert, R.S. Wittman, (2013) *Coupling the Mixed Potential and Radiolysis Models for Used Fuel Degradation*, FCRD-UFD-2013-000290, M3FT-PN0806058.

Bouniol, P., (2010) *The influence of iron on water radiolysis in cement-based materials*, Journal of Nuclear Materials **403**,167–183.

De Laat , Joseph, and Gallard, Herve, (1999) *Catalytic Decomposition of Hydrogen Peroxide by Fe(III) in Homogeneous Aqueous Solution: Mechanism and Kinetic Modeling* Environ, Sci. Technol., **33**, 2726-2732.

Fenton, H.J.H. (1894). *Oxidation of tartaric acid in presence of iron*, J. Chem. Soc., Trans. 65 (65): 899–911.

Jerden, J., Frey, K., Cruse, T., and Ebert, W. (2013). *Waste Form Degradation Model Status Report: ANL Mixed Potential Model, Version 1. Archive*. FCRD-UFD-2013-000057.

Jerden, James L., Frey, Kurt, and Ebert, William (2015), *A multiphase interfacial model for the dissolution of spent nuclear fuel*, Journal of Nuclear Materials, 462: 135-146.

Sassani et al., 2012 *Integration of EBS Models with Generic Disposal System Models*, U.S. Department of Energy, Used Fuel Disposition Campaign milestone report: M2FT-12SN0806062, September, 7 2012

Shoesmith, D.W., Kolar, M., and King, F. (2003). A Mixed-Potential Model to Predict Fuel (Uranium Dioxide) Corrosion Within a Failed Nuclear Waste Container, *Corrosion*, 59, 802-816.

Wittman RS and EC Buck. 2012. “Sensitivity of UO<sub>2</sub> Stability in a Reducing Environment on Radiolysis Model Parameters.” In *Actinides and Nuclear Energy Material, MRS Spring 2012 Proceedings*, vol. 1444, 3-8, ed. D Andersson, et al. Cambridge University Press, Cambridge, United Kingdom. DOI:10.1557/opl.2012.1449.

## APPENDIX A: Reaction Listing for Full RM

Equilibrium constants:

H2O <--> H+ + OH- : RKeq(2) = 10<sup>(-13.999)</sup>  
H2O2 <--> H+ + HO2- : RKeq(3) = 10<sup>(-11.65)</sup>  
OH <--> H+ + O- : RKeq(4) = 10<sup>(-11.9)</sup>  
HO2 <--> H+ + O2- : RKeq(5) = 10<sup>(- 4.57)</sup>  
H <--> H+ + E- : RKeq(6) = 10<sup>(- 9.77)</sup>

Reactions	Rate constants (M <sup>-n</sup> /s)
1 H+ + OH- = H2O	1.4d11
2 H2O = H+ + OH-	rk( 2) = rk( 1)*RKeq(2)
3 H2O2 = H+ + HO2-	rk( 3) = rk( 4)*RKeq(3)
4 H+ + HO2- = H2O2	5.0d10
5 H2O2 + OH- = HO2- + H2O	1.3d10
6 HO2- + H2O = H2O2 + OH-	rk( 6) = rk( 5)*RKeq(2)/RKeq(3)
7 E- + H2O = H + OH-	1.9d1
8 H + OH- = E- + H2O	2.2d7
9 H = E- + H+	rk( 9) = rk(10)*RKeq(6)
10 E- + H+ = H	2.3d10
11 OH + OH- = O- + H2O	1.3d10
12 O- + H2O = OH + OH-	rk(12) = rk(11)*RKeq(2)/RKeq(4)
13 OH = O- + H+	rk(13) = rk(14)*RKeq(4)
14 O- + H+ = OH	1.0d11
15 HO2 = O2- + H+	rk(15) = rk(16)*RKeq(5)
16 O2- + H+ = HO2	5.0d10
17 HO2 + OH- = O2- + H2O	5.0d10
18 O2- + H2O = HO2 + OH-	rk(18) = rk(17)*RKeq(2)/RKeq(5)
19 E- + H2O2 = OH + OH-	1.1d10
20 E- + O2- + H2O = HO2- + OH-	1.3d10
21 E- + HO2 = HO2-	2.0d10
22 E- + O2 = O2-	1.9d10
23 H + H2O = H2 + OH	1.1d1
24 H + H = H2	7.8d9
25 H + OH = H2O	7.0d9
26 H + H2O2 = OH + H2O	9.0d7
27 H + O2 = HO2	2.1d10
28 H + HO2 = H2O2	1.8d10
29 H + O2- = HO2-	1.8d10
30 OH + OH = H2O2	3.6d9
31 OH + HO2 = H2O + O2	6.0d9
32 OH + O2- = OH- + O2	8.2d9
33 OH + H2 = H + H2O	4.3d7
34 OH + H2O2 = HO2 + H2O	2.7d7
35 HO2 + O2- = HO2- + O2	8.0d7
36 H2O2 = OH + OH	2.25d-7
37 OH + HO2- = HO2 + OH-	7.5D9
38 HO2 + HO2 = H2O2 + O2	7.0d5
38 HO2 + HO2 = H2O2 + O2	7.0d5
39 Fe+3 + H2O = FeOH+2 + H+	1d5
40 FeOH+2 + H+ = Fe+3 + H2O	0.d0
41 Fe+3 + H2O + H2O = Fe(OH)2+ + H+ + H+	1d5
42 Fe(OH)2+ + H+ + H+ = Fe+3 + H2O + H2O	0.d0
43 Fe+3 + Fe+3 + H2O + H2O = Fe2(OH)2+4 + H+ + H+	1d5
44 Fe2(OH)2+4 + H+ + H+ = Fe+3 + Fe+3 + H2O + H2O	0.d0
45 Fe+3 + H2O2 = Fe(HO2)+2 + H+	1d5
46 Fe(HO2)+2 + H+ = Fe+3 + H2O2	0.d0
47 FeOH+2 + H2O2 = Fe(OH)(HO2)+ + H+	1d5
48 Fe(OH)(HO2)+ + H+ = FeOH+2 + H2O2	0.d0
49 Fe(HO2)+2 = Fe+2 + HO2	2.7e-3
50 Fe(OH)(HO2)+ = Fe+2 + HO2 + OH-	2.7e-3
51 Fe+2 + H2O2 = Fe+3 + OH + OH-	63.0

52	$\text{Fe}^{+2} + \text{OH} = \text{Fe}^{+3} + \text{OH}^-$	3.2e8
53	$\text{Fe}^{+2} + \text{HO}_2 = \text{Fe}(\text{HO}_2)^{+2}$	1.2e6
54	$\text{Fe}^{+2} + \text{O}_2^- + \text{H}^+ = \text{Fe}(\text{HO}_2)^{+2}$	1.0e7
55	$\text{Fe}^{+3} + \text{HO}_2 = \text{Fe}^{+2} + \text{O}_2 + \text{H}^+$	1.9e3
56	$\text{FeOH}^{+2} + \text{HO}_2 = \text{Fe}^{+2} + \text{O}_2 + \text{H}_2\text{O}$	1.9e3
57	$\text{Fe}(\text{OH})_2^{+2} + \text{HO}_2 = \text{Fe}^{+2} + \text{O}_2 + \text{H}_2\text{O} + \text{OH}^-$	1.9e3
58	$\text{Fe}^{+3} + \text{O}_2^- = \text{Fe}^{+2} + \text{O}_2$	5e7
59	$\text{Fe}_2(\text{OH})_2^{+4} + \text{O}_2^- = 2\text{Fe}^{+2} + \text{O}_2 + \text{OH}^-$	5e7
60	$\text{Fe}(\text{OH})_2^{+2} + \text{O}_2^- = \text{Fe}^{+2} + \text{O}_2 + \text{OH}^- + \text{OH}^-$	5e7